

# THE INTERNATIONAL JOURNAL OF SCIENCE & TECHNOLEDGE

## Combined Convection Flow through Inclined Square Enclosure with a Sliding Corrugated Hot Top Surface

**Jeremiah Rioba Ogata**

Teacher, Igorera Secondary School, Kisii County, Kenya

**Johana K. Sigey**

Director, Jomo Kenyatta University of Agriculture and Technology, Kenya

**Dr. Jeconia A. Okelo**

Senior Lecturer, Department of Pure and Applied Mathematics

Assistant Supervisor, Jomo Kenyatta University of Agriculture and Technology, Kenya

**Dr. James M. Okwoyo**

Lecturer, University of Nairobi, Kenya

**Dr. Kang'ethe Giterere**

Lecturer, Jomo Kenyatta University of Agriculture and Technology, Kenya

### **Abstract:**

*This research project was a study of combined convection flow through inclined square enclosure with a sliding corrugated hot top surface. The hot isothermal top wall was corrugated with three undulations and the wave amplitude was 0.1 and was sliding at constant velocity. The bottom wall was fixed and kept at isothermal cold temperature. The other side walls were thermally insulated. The inclination angle was kept constant at 100 with the enclosure filled with water as a working fluid. The velocity profile and temperature distribution was obtained using MATLAB. The partial differential equations governing water velocity and temperature distribution were solved numerically using Finite Difference Method and the result were discussed and presented in tables and graphs. The effects of Richardson number and Reynolds number on velocity flow and temperature distribution in the enclosure were analyzed with Prandtl number kept constant.*

**Keywords:** Richardson number, Reynolds number, partial differential equations, finite difference method, The hot isothermal top wall, and a sliding corrugated hot top surface.

## **1. Introduction**

### *1.1. Background*

Heat transfer involves flow of heat and temperature. Heat flow is the movement of thermal energy from one point to another due to temperature difference. Temperature is the amount of thermal energy available. A fluid is any substance that flows. Convection is the transfer of energy by movement of a substance. Convection can be natural or forced. Natural convection is when the movement of substance results from a difference in density for example as with air around a fire.

The fundamental problem of combined convection heat transfer has received considerable attention from researchers. Combined convection is due to shear flow caused by the movement of one of the walls of the cavity. Combined convection flow and heat transfer are present in many transport processes and engineering devices. Some examples of combined convection flows can be found in atmospheric flows, nuclear reactors, solar energy storage, refrigeration devices, lubrication technologies and heat exchangers.

Forced convection is typically used to increase the rate of heat exchange. Forced convection is the movement of fluid over a surface or a tube by external means such as a pump or fan as in some hot air and hot water heating systems. The difference in temperature brings about the changes in cooling and heating effects of a fluid. The boiling of water for instance is due to convection currents.

It should be noted that heat transfer is sustained by both bulk motion of fluid and molecular motion within the boundary layer. Specific heat, density, thermal conductivity and viscosity determine the convection of heat. The velocity profile of the fluid flow is influenced by viscosity. Viscosities of all fluids depend on temperature. The viscosity increases for gases and decreases for liquids as temperature increases. The higher the velocity of the flowing fluid, the higher the rate of heat transfer rate. In case of combined convection, one could often like to know how much of the convection is due to external constraints, such as the fluid velocity and how much is due to free convection occurring in the system. The relative magnitude of thermal buoyancy force and acceleration force determine which form of convection dominates. If thermal buoyancy is much stronger than acceleration force, then forced convection

may be neglected whereas if acceleration force is much stronger than thermal buoyancy then free convection may be neglected. If their relative magnitude is of order one, and then both the free and forced convection is dominant.

### 1.2. Literature Review

Combined convection flow through inclined square with a sliding corrugated hot top surface is of great importance in both natural and scientific applications. This type of flow is applied in high performance boilers, chemical catalytic reactors, solar collectors, power plants, heat exchangers, refrigeration devices, lubrication technologies, drying technologies, food processing and cooling of electronic systems.

Different investigations have been performed to deal with an enclosure fluid flow and heat transfer by considering various boundary and geometric configurations. Mohamed (2013) studied a numerical simulation of mixed radiation and forced convection heat transfer in a lid-driven cavity filled with participating media. He realized that, temperature contours, mid-plan temperature distribution and overall heat flux distributions on the walls were obtained for different parameters like the Reynolds number, scattering coefficient and location of heat generation zone. It was found that these parameters have great effects on thermal behavior of such systems.

Obayedullah *et al* (2013), studied natural convection in a rectangular cavity having internal energy sources and electrically conducting fluid with sinusoidal temperature at the bottom wall. They noted that, internal Rayleigh number affects the flow and temperature field inside the enclosure significantly, an increasing rate of heat within the cavity due to the increase of internal Rayleigh number leads to form a secondary cell within the cavity and increases in size until it occupies half of the enclosure, increment of internal Rayleigh number enhances the rate of heat transfer, the convective current in the enclosure is reduced as the Hartmann number increases and because of this the size of the secondary cell is reduced and with the increase of the strength of magnetic field the average Nusselt number decreases.

Hussain (2009), Studied the internal heat transfer by natural convection through an inclined and modified square enclosure with a triangular top wall. He noted the following: when the inclination angle is  $0^\circ$  and the Rayleigh numbers are low, the buoyancy force effect is small and the convection heat transfer contribution is small, as Rayleigh number increases, the vortices shape becomes irregular and making a large convection heat transfer contribution, when the inclination angle is  $0^\circ$  the isotherm contours refer that the thermal field lines are almost linear and symmetrical at the upper part of the enclosure, so the diffusion heat transfer is dominated while the convection heat transfer is dominated at the lower part of the enclosure, when the Rayleigh number increases, the isotherms become non-symmetry, uniform horizontally and linear vertically at the upper part of the enclosure, when the inclination angle is increased, the

effect of inclination angle is small when the Rayleigh number is low but when the Rayleigh number increases the fluid flow nature has a clear different behaviour, when the Rayleigh number is low, there is a primary recirculation vortex which covers most of the enclosure size. At  $Ra = 10^6$ , a two non-uniform recirculating vortices of different shape and opposite directions can be noticed, when  $E/L$  ratio increases with the increase in the Rayleigh number and the inclination angle, the spacing near the triangular inclined top walls decreases and the flow field enlarge to cover all the enclosure zone and when the  $E/L$  ratio is high, the average Nusselt number increases with the increase in the Rayleigh number and the inclination angle.

Hussain S.H (2010), studied combined convection flow through inclined rectangular enclosure with sliding wavy hot top surface. He found out that, forced convection is dominant when Richardson number is small; the enclosure inclination angle has a little effect in the streamlines and isotherms. The total heat transfer process is insensitive to the inclination angle when the Richardson number is small. When the Richardson number is unity, then combined convection is the dominant behaviour. When the Richardson number is large, then free convection is dominant behaviour and the effect of the enclosure inclination angle has an important effect on the thermal and hydrodynamic flow fields. He also noted that, at any location the local Nusselt number increases with the inclination angle. For large values of Richardson number, the local Nusselt number is greater for the inclined enclosures than for non-inclined one.

Mohamed *et al* (2012), studied numerical simulation of double-diffusive natural convective flow in an inclined rectangular enclosure in the presence of magnetic field and heat source. They noted that, for lower values of the thermal Rayleigh number, the conduction regime was dominant, increasing the source term in the momentum equation, by increasing the thermal Rayleigh number, always led to increases on the heat and mass transfer performance of the enclosure. They also observed that, the inclination angle affects the buoyancy forces in the enclosure, the maximum and minimum average Nusselt and Sherwood numbers were at inclination angle,  $\gamma = 150^\circ$  and  $75^\circ$  respectively. Further noticed that, there was effect of thermal Rayleigh number on the horizontal cavity by the increase in the number of convection rolls developed within the cavity.

Mohamed *et al* (2013), studied numerical simulation of double diffusive laminar mixed convective ...in shallow inclined cavities with moving lid. They realized that, the flow field is characterized by a primary circulating bubble with its place depends on the direction of the moving lid. Furthermore, high  $Le$  is found to have insignificant impact on the heat transfer rate. They also noted that, an increase in the absolute value of buoyancy ratio number,  $N$ , enhanced the estimated Nusselt number and the Sherwood number for both cases of lid movement. Arash *et al* (2014). Using nanofluid in liquid driven shallow enclosure at particular Richardson number: Investigate the effect of velocity ratio. They concluded that, while the velocity ratio increases in all cases, with the exception of the very low values of the Reynolds number, the vortex in the vicinity of the right wall enhances and the heat transfer ratio increases, there is a very sharp increase in the Nusselt number and subsequently in the heat transfer ratio while the Richardson number increases at a constant velocity ratio and adding the nanoparticles to the base fluid, results in increasing the average Nusselt number. It also leads to increase in the rate of heat transfer.

Rehena *et al* (2014), Effect of Prandtl number on 3D heat transfer through a solar collector. They found out that, the configuration of the streamlines plot of heat and flow fields of the solar flat plate collector was significantly depended upon  $Pr$ , the water-Cu nanofluid with the highest  $Pr$  was the most effective in enhancing performance of heat transfer rate, mean temperature devalues for both fluids with growing values of  $Pr$ , collector efficiency was obtained higher for the highest Prandtl number and outlet temperature of nanofluid rises due to escalating  $Pr$ .

Elif B.O (2010) investigated mixed convection in an inclined lid-driven enclosure with a constant flux heater using differential quadrature (dq) method. He noticed that, the differential quadrature (DQ) technique provides accurate results for the problems of mixed convection. He also noted that, the flow field and temperature distribution are also significantly influenced by the inclination angle. The rate of influence depends highly on the value of Richardson number. For flow with low values of Richardson number (e.g.  $Ri = 0.1$ ), the effect of inclination angle can be omitted. The influence of the inclination angle enhances with increase of Richardson number. Maximum effect of the inclination angle was observed for a cavity with  $Ri = 10$  in which natural convection mode of heat transfer is dominant. Finally, he realized that, for cavity with  $Ri = 10$  and  $\omega = 180^\circ$ , the heat from the heated wall to cold moving lid is transferred via conduction and consequently  $Nu \approx 1$ .

Kumar *et al* (2013) investigated mixed convection heat transfer in a lid-driven cavity with wavy bottom surface. They found that the heat transfer mechanisms and the flow characteristics inside the cavity are strongly dependent on the number of undulations, Grashof number and Reynolds number. When the ratio of Grashof number and square of Reynolds number (Richardson number) is greater or equal to unity then the streamline contours over the whole cavity region is occupied by several primary vortex. In that case, heat transfer was mainly through conduction except the upper portion of the cavity. The isotherms were not affected by the variation of undulation numbers at the bottom surface except the vicinity of the wavy bottom surface. The skin friction and local Nusselt number increased with increasing values of Reynolds number for any values of undulation number. Finally, the prediction of the local and average Nusselt number was found to increase with larger values of Grashof number and higher amplitude of the wavy surface. Thus, the wavy lid-driven cavity can be considered as an effective heat transfer mechanism at larger wavy surface amplitudes and higher Grashof number.

Salah U.K.M & Litan K.S (2015) analyzed numerical solutions of 2-D incompressible driven cavity flow with wavy bottom surface. The two found out that, wall undulation affects the flow in the lid driven square cavity. Employing the number of undulations at bottom surface, the skin friction increases. The skin friction becomes highest at the upper peak point and it becomes lowest at the lower peak point. Sigey *et al* (2011) who studied buoyancy driven free convection turbulent heat transfer in an enclosure. They investigated a three-dimensional enclosure containing a convective heater built into one wall having a window in same wall. The results were that three regions a cold upper region, a hot region in the area between and a warm lower region.

Ahmed (2010) predicted numerically free convection phenomenon through a rectangular inclined cavity filled with a porous media. The vortices (or convection currents) are formed and a higher fluid circulation is found in the flow domain due to stronger free convection effects. The number of convective vortices or cells increases with increasing Rayleigh number. From an examination of the isotherms (dimensionless temperature lines), it is observed that for small values of Rayleigh number, convective motion is first observed near the lower corners of the cavity. As Rayleigh number increases, the temperature gradient in this region increases, thus increasing the heat transfer in this region. Stronger circulation occurs at higher Rayleigh number. The circulations are greater near the center and least at the wall due to no-slip boundary conditions. The average Nusselt number increases when the values of Rayleigh number and the inclination angle increase.

Stiriba *et al* (2010) carried out a numerical study of three-dimensional laminar mixed convection past an open cavity. They found out that the flow exhibits a three-dimensional structure and becomes steady for  $Re = 100$  with  $Ri \leq 100$  and  $Re = 1000$  with  $Ri \leq 0.1$ . The forced flow dominates the flow transport mechanism and large recirculation zone from inside the enclosure which results in heat transfer by conduction and in this case the Nusselt number increases slightly. For both Reynolds and Richardson numbers, the natural convection comes into play and pushes the recirculation zone further upstream. Ntabo *et al* (2015) investigated the effect of electromagnetic field on forced convective heat transfer in a vertical wavy channel divided by conductive partition was studied. It was found out that, as the Reynolds number increased, velocity of the fluid flow was enhanced. This implies that the inertial forces dominated over the viscous forces. It was also seen that reduction of electric load reduction promotes the fluid flow. It was further indicated that, the temperature is increased with increase in wall temperature ratio and Prandtl number. Finally, it was noted that, the wavy wall enhances the flow and temperature distribution. Khanafer *et al* (2002) studied mixed convection heat transfer in two-dimensional open ended enclosure. Their results are as follows: the lower and upper Nusselt numbers increase almost linearly with the Reynolds numbers, for low Grashof number, the results show that the lower average Nusselt number is the highest for the  $45^\circ$  flow angle of attack. The upper Nusselt number is found to be highest for the  $90^\circ$  flow angle of attack. Hasanuzzaman M. and Mohammed A. (2007) studied heat transfer by natural convection through V corrugated plates. They noted the following: heat transfer rate increases with the decrease of inlet water temperature. Heat transfer rate increases with the increase of input power and mass flow rate of water. For low input of power, the increment of heat transfer is high mass flow rate of cooling water causes low increment of heat flux. For high input power constant increment of heat transfer can be observed with the increase of mass flow rate of cooling water. Onchaga *et al* (2013) studied turbulent Natural Convection of Heat with Localized Heating and Cooling on Adjacent Vertical Walls in an Enclosure. The results show that in an enclosure environment, the natural turbulence flow plays an important role in the temperature distribution. Regions of varying temperatures are created either across the room or in an upward direction. This helps in keeping of some items at the stated temperature.

Salam *et al* (2011) studied natural convection in a square inclined enclosure with vee corrugated side walls subjected to constant flux heating from below. They noted that, when the inclination angle is zero; the flow field begins to grow along the vertical mid-plane and

then stops near the adiabatic top wall. In view of the forgoing literature review, it has been noted that, the angle inclination is varied but in this case, the angle of inclination of the cavity with the horizontal will be constant. Combined convection flow through inclined square enclosure with sliding corrugated hot top surface has not been fully exhausted.

### 1.3. Statement of the Problem

This research was aimed at studying combined convection flow through inclined square enclosure with a sliding corrugated hot top surface. The inclination angle was kept constant. Effects of variation of Richardson number and Reynolds number on temperature distribution and velocity profile was analyzed. These parameters were varied and Finite Difference method was used to solve velocity and energy equations.

### 1.4. Justification of the Study

Effect of change of Ri and Re will aid in manufacturing industries for good manufacture and output performance of atmospheric flows, heat exchangers, nuclear reactors, solar energy storage, heat rejection systems, refrigeration devices, drying technologies, food processing, cooling of electronic systems and lubrication technologies.

### 1.5. General Objective

The general objective of this research was to study combined convection flow through inclined square enclosure with a sliding corrugated hot top surface.

### 1.6. Specific Objectives

- i. To obtain the velocity profiles and temperature distribution in the square enclosure caused by combined convection flow.
- ii. To investigate the effects of Ri and Re on the combined convection flow.

### 1.7. Null Hypothesis

Richardson number and Reynolds number do not influence heat transfer, temperature distribution and velocity profiles in a square enclosure with a sliding corrugated hot top surface.

## 2. Mathematical Formulations

### 2.1. Geometry of the Problem

The heat transfer and the fluid flow in a two-dimensional inclined square enclosure of width (L) and height (L) was considered as shown in the schematic diagram of **Fig. 1** shown below.

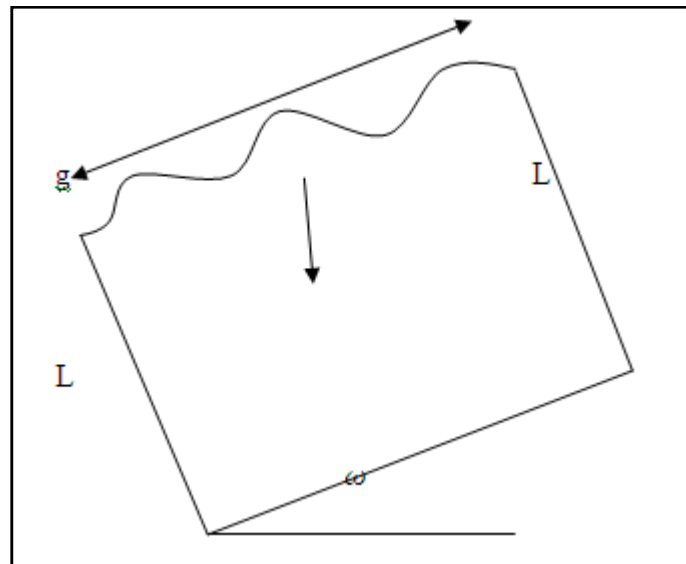


Figure 1: Configuration of the square cavity

The aspect ratio ( $A_s$ ) of the enclosure was 1 and it was defined as  $A_s = L/L$ . The top wall of the enclosure was considered corrugated with three undulations where the wave amplitude was 0.1 and sliding at a constant speed,  $U_{Lid}$  and was maintained at a uniform hot temperature  $T_h$  while the bottom wall was maintained at a uniform cold temperature  $T_c$ . The two other remaining walls were considered thermally insulated. The fluid inside the enclosure was assumed to be water ( $Pr = 6$ ) where the viscous dissipation effects were considered negligible, and the fluid flow was considered to be laminar and steady. The fluid properties were assumed constant except for the density variation in the buoyancy term which was treated according to Boussinesq approximation.

The enclosure was inclined at an angle  $\omega$  which was  $10^\circ$ . The flow field was produced by the combined effect of shear force resulting from the top hot corrugated wall movement and the buoyancy force resulting from the hot temperature at the same wall. The problem was solved numerically using a finite difference method and the results were presented in tables and graphs. The effect of Ri and Re numbers on the velocity and temperature of the fluid were investigated. The laminar internal two-dimensional flow and the thermal field inside the enclosure were described by the Navier–Stokes and the energy equations, respectively.

## 2.2. Governing Equations

The general governing equations, that is, continuity, momentum and energy equations are as below. (Mohamed A.T, 2013)

$$\frac{\partial U}{\partial X} + \frac{\partial V}{\partial Y} = 0 \quad (1)$$

$$\rho \left( U \frac{\partial U}{\partial X} + V \frac{\partial U}{\partial Y} \right) = -\frac{\partial P}{\partial X} + \rho g + \mu \nabla^2 U \quad (2)$$

$$\rho \left( U \frac{\partial V}{\partial X} + V \frac{\partial V}{\partial Y} \right) = -\frac{\partial P}{\partial Y} + \rho g + \mu \nabla^2 V \quad (3)$$

$$\rho C_p \left( U \frac{\partial \theta}{\partial X} + V \frac{\partial \theta}{\partial Y} \right) = -\frac{\partial P}{\partial X} + K \nabla^2 T \quad (4)$$

The above governing equations were transformed into dimensionless forms by using the following dimensionless variables (Sharif, 2007):

$$\theta = \frac{T - T_c}{T_h - T_c}, X = \frac{x}{L}, Y = \frac{y}{L} \quad (5)$$

$$U = \frac{u}{U_{Lid}}, V = \frac{v}{U_{Lid}}, P = \frac{P}{\rho U_{Lid}^2} \quad (6)$$

The dimensionless forms of the governing equations of steady internal laminar combined convection were expressed in the following forms (Sharif, 2007):

### 2.2.1. Continuity Equation

$$\frac{\partial U}{\partial X} + \frac{\partial V}{\partial Y} = 0 \quad (7)$$

### 2.2.2. Momentum Equations

$$U \frac{\partial U}{\partial X} + V \frac{\partial U}{\partial Y} = -\frac{\partial P}{\partial X} + \frac{1}{Re} \nabla^2 U + \left( \frac{Gr}{Re^2} \theta \right) \sin(\omega) \quad (8)$$

$$U \frac{\partial V}{\partial X} + V \frac{\partial V}{\partial Y} = -\frac{\partial P}{\partial Y} + \frac{1}{Re} \nabla^2 V + \left( \frac{Gr}{Re^2} \theta \right) \cos(\omega) \quad (9)$$

### 2.2.3. Energy Equation

$$U \frac{\partial \theta}{\partial X} + V \frac{\partial \theta}{\partial Y} = -\frac{\partial P}{\partial X} + \frac{1}{Re Pr} \nabla^2 \theta \quad (10)$$

where  $X$  and  $Y$  are the dimensionless coordinates measured along the enclosure normal sides with left lower corner of the origin.  $U$  and  $V$  being the dimensional velocity components along  $x$  and  $y$  axes. Also,  $\theta$  is the dimensionless temperature,  $P$  is the dimensionless pressure,  $Pr$  is the Prandtl number,  $Re$  is the Reynolds number and  $Gr$  is the Grashof number. The previous dimensionless numbers are defined as (Bejan, and Kraus, 2003): -

$$Pr = \frac{\nu}{\alpha}, Re = \frac{U_{Lid} L}{\nu} \text{ and } Gr = \frac{g \beta (T_h - T_c) L^3}{\nu^2} \quad (11)$$

where  $\beta$  is the volumetric coefficient of thermal expansion,  $\nu$  is the kinematic viscosity,  $\alpha$  is the thermal diffusivity and  $g$  is the gravitational acceleration. Also, Rayleigh number  $Ra$ , and Richardson Number,  $Ri$ , are defined by (Bejan, and Kraus, 2003):-

$$Ra = \frac{g \beta (T_h - T_c) L^3 Pr}{\nu^2} \text{ and } Ri = \frac{Gr}{Re^2} \quad (12)$$

Richardson number,  $Ri$  is a measure of the relative strength of the natural convection and forced convection for a particular problem.

The shape of the hot corrugated top wall surface profile was assumed to obey the following equation (Al-Amiri *et al.*, 2007):

$$Y = \delta (1 - \cos(2 \lambda \pi X)) + 1 \quad (13)$$

where  $\delta$  is the dimensionless amplitude of the corrugated surface and  $\lambda$  is the number of undulations. The heat transfer rate is determined at the hot and cold walls and is expressed in terms of local and average Nusselt number as follows (Sharif, 2007):

$$Nu_x = -\left( \frac{\partial \theta}{\partial Y} \right)_{Y=0.1} \quad (14)$$

$$Nu_{av} = \frac{1}{A_s} \int_0^{A_s} Nu_x dX \quad (15)$$

Subject to the following boundary conditions:

i. The top wall is corrugated and sliding at a constant velocity ( $U_{Lid}$ ) and it is kept at a uniform hot temperature ( $T_h$ ) so:

$$Y = \delta (1 - \cos(2 \lambda \pi X)) + 1, \theta = 1, U = U_{Lid} \text{ and } V = 0 \quad (16)$$

ii. The bottom wall is kept at a uniform cold temperature ( $T_c$ ) so:

$$Y = 0, \theta = 0 \text{ and } U = V = 0 \quad (17)$$

iii. The left side wall is thermally insulated, so:  $X = 0, \frac{\partial \theta}{\partial Y} = 0$  and  $U = V = 0$  (18)

iv. The right side wall is thermally insulated, so:  $X = 1, \frac{\partial \theta}{\partial Y} = 0$  and  $U = V = 0$  (19)

### 2.3. Assumptions

- i. The fluid inside the enclosure was assumed to be water, ( $Pr = 6$ ), since water is less viscous
- ii. Viscous dissipative effects were considered negligible since viscosity of water is very small.
- iii. The fluid flow was considered to be laminar and steady,  $Re < 2300$ .

## 3. Method of Solution

### 3.1. Introduction

In this section, the method and procedure of solving the problem is discussed

### 3.2. Computational Procedure

In this study a Crank-Nicolson numerical scheme be develop and Finite Difference Method will be used to solve the momentum and energy equations. The method obtains a finite system of linear or nonlinear algebraic equations from the momentum and energy equations Partial Differential Equation by discretizing the given equation and coming up with the numerical schemes analogues to the equation, in our case the momentum and energy equations. We solve the equations subject to the given boundary conditions. MATLAB software is used to generate solution values in this study.

### 3.3. Discretization of the Governing Equations

Considering momentum and energy equations;

$$U \frac{\partial U}{\partial X} + V \frac{\partial U}{\partial Y} = -\frac{\partial p}{\partial X} + \frac{1}{Re} \left( \frac{\partial^2 U}{\partial X^2} + \frac{\partial^2 U}{\partial Y^2} \right) + \left( \frac{Gr}{Re^2} \theta \right) \sin(w) \quad (20)$$

$$U \frac{\partial V}{\partial X} + V \frac{\partial V}{\partial Y} = -\frac{\partial P}{\partial X} + \frac{1}{Re} \left( \frac{\partial^2 V}{\partial X^2} + \frac{\partial^2 V}{\partial Y^2} \right) + \left( \frac{Gr}{Re^2} \theta \right) \cos(w) \quad (21)$$

$$U \frac{\partial \theta}{\partial X} + V \frac{\partial \theta}{\partial Y} = -\frac{\partial p}{\partial X} + \frac{1}{Re Pr} \left( \frac{\partial^2 \theta}{\partial X^2} + \frac{\partial^2 \theta}{\partial Y^2} \right) \quad (22)$$

In the current investigation, the Richardson number was defined as;

$$Ri = \frac{Gr}{Re^2}$$

where Grashof number and Reynolds number are defined as;

$$Gr = \frac{g \beta (T_h - T_c) L^3}{\nu^2}, Re = \frac{U_{lid} L}{\nu}$$

### 3.4. Horizontal Velocity

Using Crank-Nicolson scheme,  $u_i$  is replaced by forward difference approximation while  $u_{xx}$  is replaced by central difference approximation average of the  $j^{\text{th}}$  level and the  $(j+1)^{\text{th}}$  level the equation (20) becomes

$$\left[ \frac{U_{i+1,j} - U_{i,j}}{\Delta x} \right] = \frac{1}{2 \times 10^2} \left[ \frac{U_{i+1,j} - 2U_{i,j} + U_{i-1,j}}{(\Delta x)^2} + \frac{U_{i+1,j+1} - 2U_{i,j+1} + U_{i-1,j+1}}{(\Delta x)^2} \right] + \left[ \frac{U_{i,j+1} - 2U_{i,j} + U_{i,j-1}}{(\Delta y)^2} \right] + (0.8 \times 1) \sin 10^\circ \quad (23)$$

We investigate the effect of Re, Ri on the fluid velocity. Taking  $\Delta x = \Delta y = 0.1$ ,  $Re = 10^2, 10, 1$   $Ri = 0.8, 1, 2$  and  $P = 0, V = 0, \theta = 1, U = 1$ , we get the scheme

$$0.9U_{i+1,j} - 1.0U_{i,j} - 0.1U_{i-1,j} = 0.1U_{i,j-1} + U_{i,j+1} + 0.0694593 \quad (24)$$

Taking  $i = 1, 2, 3, \dots, 8$  and  $j = 1$  we form the following systems of linear algebraic equations

$$\begin{aligned}
 0.9U_{2,1} - 1.0U_{1,1} - 0.1U_{0,1} &= 0.1U_{1,0} + U_{1,2} + 0.0694593 \\
 0.9U_{3,1} - 1.0U_{2,1} - 0.1U_{1,1} &= 0.1U_{2,0} + U_{2,2} + 0.0694593 \\
 0.9U_{4,1} - 1.0U_{3,1} - 0.1U_{2,1} &= 0.1U_{3,0} + U_{3,2} + 0.0694593 \\
 0.9U_{5,1} - 1.0U_{4,1} - 0.1U_{3,1} &= 0.1U_{4,0} + U_{4,2} + 0.0694593 \\
 0.9U_{6,1} - 1.0U_{5,1} - 0.1U_{4,1} &= 0.1U_{5,0} + U_{5,2} + 0.0694593 \\
 0.9U_{7,1} - 1.0U_{6,1} - 0.1U_{5,1} &= 0.1U_{6,0} + U_{6,2} + 0.0694593 \\
 0.9U_{8,1} - 1.0U_{7,1} - 0.1U_{6,1} &= 0.1U_{7,0} + U_{7,2} + 0.0694593 \\
 0.9U_{9,1} - 1.0U_{8,1} - 0.1U_{7,1} &= 0.1U_{8,0} + U_{8,2} + 0.0694593 \\
 0.9U_{10,1} - 1.0U_{9,1} - 0.1U_{8,1} &= 0.1U_{9,0} + U_{9,2} + 0.0694593 \\
 0.9U_{11,1} - 1.0U_{10,1} - 0.1U_{9,1} &= 0.1U_{9,0} + U_{10,2} + 0.0694593
 \end{aligned}$$

The above algebraic equations can be written in matrix form as when  $u(x,0)=0$  and  $u(x,2) = e^{-x}$

$$\begin{bmatrix}
 3.4 & -0.4 & 0 & 0 & 0 & 0 & 0 & 0 & 0 & 0 \\
 -1 & 3.4 & -0.4 & 0 & 0 & 0 & 0 & 0 & 0 & 0 \\
 0 & -1 & 3.4 & -0.4 & 0 & 0 & 0 & 0 & 0 & 0 \\
 0 & 0 & -1 & 3.4 & -0.4 & 0 & 0 & 0 & 0 & 0 \\
 0 & 0 & 0 & -1 & 3.4 & -0.4 & 0 & 0 & 0 & 0 \\
 0 & 0 & 0 & 0 & -1 & 3.4 & -0.4 & 0 & 0 & 0 \\
 0 & 0 & 0 & 0 & 0 & -1 & 3.4 & -0.4 & 0 & 0 \\
 0 & 0 & 0 & 0 & 0 & 0 & -1 & 3.4 & -0.4 & 0 \\
 0 & 0 & 0 & 0 & 0 & 0 & 0 & -1 & 3.4 & -0.4 \\
 0 & 0 & 0 & 0 & 0 & 0 & 0 & 0 & -1 & 3.4
 \end{bmatrix}
 \begin{bmatrix}
 U_{11} \\
 U_{21} \\
 U_{31} \\
 U_{41} \\
 U_{51} \\
 U_{61} \\
 U_{71} \\
 U_{81} \\
 U_{91} \\
 U_{101}
 \end{bmatrix}
 =
 \begin{bmatrix}
 1.53383 \\
 0.3047946 \\
 0.212464 \\
 0.1877749 \\
 0.17197094 \\
 0.17938052 \\
 0.170371182 \\
 0.169794762 \\
 0.169582709 \\
 0.169504699
 \end{bmatrix}
 \tag{25}$$

Solving the above matrix equation, we get the solutions for changing Ri

Ri=0.8 Ri=1 Ri=2

$$\begin{aligned}
 U_{1,1} &= 0.4814504 & U_{1,1} &= 0.7239203 & U_{1,1} &= 0.7845907 \\
 U_{2,1} &= 0.248926 & U_{2,1} &= 0.5657554 & U_{2,1} &= 0.6446009 \\
 U_{3,1} &= 0.15074 & U_{3,1} &= 0.4901801 & U_{3,1} &= 0.5745702 \\
 U_{4,1} &= 0.1107173 & U_{4,1} &= 0.4570723 & U_{4,1} &= 0.5431538 \\
 U_{5,1} &= 9.480941 \times 10^{-2} & U_{5,1} &= 0.4432731 & U_{5,1} &= 0.5298703 \\
 U_{6,1} &= 8.859417 \times 10^{-2} & U_{6,1} &= 0.437693 & U_{6,1} &= 0.5244457 \\
 U_{7,1} &= 8.618175 \times 10^{-2} & U_{7,1} &= 0.4354089 & U_{7,1} &= 0.5221927 \\
 U_{8,1} &= 8.513151 \times 10^{-2} & U_{8,1} &= 0.4338612 & U_{8,1} &= 0.520521 \\
 U_{9,1} &= 8.367654 \times 10^{-2} & U_{9,1} &= 0.4278567 & U_{9,1} &= 0.513386 \\
 U_{10,1} &= 7.446507 \times 10^{-2} & U_{10,1} &= 0.3812185 & U_{10,1} &= 0.4574472
 \end{aligned}$$

### 3.5. Vertical Velocity

Discretizing the vertical velocity equation (21) becomes

$$\left[ \frac{V_{i+1,j} - V_{i,j}}{\Delta y} \right] = \frac{1}{2 \times 10^2} \left[ \frac{V_{i+1,j} - 2V_{i,j} + V_{i-1,j}}{(\Delta x)^2} + \frac{V_{i+1,j+1} - 2V_{i,j+1} + V_{i-1,j+1}}{(\Delta x)^2} \right] + \left[ \frac{V_{i,j+1} - 2V_{i,j} + V_{i,j-1}}{(\Delta y)^2} \right] + (0.8 \times 1) \cos 10^\circ
 \tag{26}$$

We investigate the effect of Re, Ri on the fluid velocity. Taking  $\Delta x = \Delta t = 0.1$ ,  $Re=10^2, 10, 1$   $Ri=0.8, 1, 2$  and  $P=0, U=0, \theta = 1, V=1$ , we get the scheme

$$3.4V_{i,j} - V_{i+1,j} - V_{i-1,j} = V_{i,j+1} + V_{i,j-1} + 3.939231
 \tag{27}$$

Taking  $i=1,2,3,\dots,8$  and  $j=1$  we form the following systems of linear algebraic equations

$$\begin{aligned}
 1.4V_{1,1} - V_{2,1} - V_{0,1} &= V_{1,2} + V_{1,0} + 3.939231 \\
 1.4V_{2,1} - V_{3,1} - V_{1,1} &= V_{2,2} + V_{2,0} + 3.939231 \\
 1.4V_{3,1} - V_{4,1} - V_{2,1} &= V_{3,2} + V_{3,0} + 3.939231 \\
 1.4V_{4,1} - V_{5,1} - V_{3,1} &= V_{4,2} + V_{4,0} + 3.939231 \\
 1.4V_{5,1} - V_{6,1} - V_{4,1} &= V_{5,2} + V_{5,0} + 3.939231 \\
 1.4V_{6,1} - V_{7,1} - V_{5,1} &= V_{6,2} + V_{6,0} + 3.939231 \\
 1.4V_{7,1} - V_{8,1} - V_{6,1} &= V_{7,2} + V_{7,0} + 3.939231 \\
 1.4V_{8,1} - V_{9,1} - V_{7,1} &= V_{8,2} + V_{8,0} + 3.939231 \\
 1.4V_{9,1} - V_{10,1} - V_{8,1} &= V_{9,2} + V_{9,0} + 3.939231 \\
 1.4V_{10,1} - V_{11,1} - V_{9,1} &= V_{10,2} + V_{10,0} + 3.939231
 \end{aligned}$$

The above algebraic equations can be written in matrix form when initial and boundary conditions  $u(x,0)=0$  and  $u(x,2)=e^{-x}$

$$\begin{bmatrix}
 3.4 & -1 & 0 & 0 & 0 & 0 & 0 & 0 & 0 & 0 \\
 -1 & 3.4 & -1 & 0 & 0 & 0 & 0 & 0 & 0 & 0 \\
 0 & -1 & 3.4 & -1 & 0 & 0 & 0 & 0 & 0 & 0 \\
 0 & 0 & -1 & 3.4 & -1 & 0 & 0 & 0 & 0 & 0 \\
 0 & 0 & 0 & -1 & 3.4 & -1 & 0 & 0 & 0 & 0 \\
 0 & 0 & 0 & 0 & -1 & 3.4 & -1 & 0 & 0 & 0 \\
 0 & 0 & 0 & 0 & 0 & -1 & 3.4 & -1 & 0 & 0 \\
 0 & 0 & 0 & 0 & 0 & 0 & -1 & 3.4 & -1 & 0 \\
 0 & 0 & 0 & 0 & 0 & 0 & 0 & -1 & 3.4 & -1 \\
 0 & 0 & 0 & 0 & 0 & 0 & 0 & 0 & -1 & 3.4
 \end{bmatrix}
 \begin{bmatrix}
 V_{11} \\
 V_{21} \\
 V_{31} \\
 V_{41} \\
 V_{51} \\
 V_{61} \\
 V_{71} \\
 V_{81} \\
 V_{91} \\
 V_{101}
 \end{bmatrix}
 =
 \begin{bmatrix}
 5.30711 \\
 4.0745663 \\
 3.9890181 \\
 3.9575466 \\
 3.94596895 \\
 3.94170975 \\
 3.9401429 \\
 3.9395665 \\
 3.9393544 \\
 3.939231
 \end{bmatrix}
 \tag{28}$$

Solving the above matrix equation, we get the solutions for changing  $Ri$   
 $Ri=0.8$   $Ri=1$   $Ri=2$

$$\begin{aligned}
 V_{1,1} &= 1.79132 & V_{1,1} &= 2.133487 & V_{1,1} &= 2.475697 \\
 V_{2,1} &= 1.95845 & V_{2,1} &= 2.404843 & V_{2,1} &= 2.851606 \\
 V_{3,1} &= 1.982112 & V_{3,1} &= 2.459012 & V_{3,1} &= 2.938959 \\
 V_{4,1} &= 1.979277 & V_{4,1} &= 2.466951 & V_{4,1} &= 2.955555 \\
 V_{5,1} &= 1.97471 & V_{5,1} &= 2.45668 & V_{5,1} &= 2.956911 \\
 V_{6,1} &= 1.97192 & V_{6,1} &= 2.46386 & V_{6,1} &= 2.955897 \\
 V_{7,1} &= 1.970272 & V_{7,1} &= 2.462347 & V_{7,1} &= 2.954533 \\
 V_{8,1} &= 1.966477 & V_{8,1} &= 2.457919 & V_{8,1} &= 2.949393 \\
 V_{9,1} &= 1.940459 & V_{9,1} &= 2.425512 & V_{9,1} &= 2.910573 \\
 V_{10,1} &= 1.729321 & V_{10,1} &= 2.161646 & V_{10,1} &= 2.59396
 \end{aligned}$$

### 3.6. Temperature

Discretizing the temperature equation (22) becomes

$$\frac{1}{10^2} \left[ \frac{\theta_{i+1,j} - 2\theta_{i,j} + \theta_{i-1,j}}{(\Delta x)^2} + \frac{\theta_{i+1,j+1} - 2\theta_{i,j+1} + \theta_{i-1,j+1}}{(\Delta x)^2} \right] + \left[ \frac{\theta_{i,j+1} - 2\theta_{i,j} + \theta_{i,j-1}}{(\Delta y)^2} \right] = 0
 \tag{29}$$

We investigate the effect of  $Re$ ,  $Ri$  on the fluid velocity. Taking  $\Delta x = \Delta y = 0.1$ ,  $Re=10^2, 10, 1$   $Ri=0.8, 1, 2$  and  $P=0, U=0, \theta = 1, V=1$ , we get the scheme

$$3.4\theta_{i,j} - \theta_{i+1,j} - \theta_{i-1,j} = \theta_{i,j+1} + \theta_{i,j-1} + 3.939231
 \tag{30}$$

Taking  $and i=1, 2, 3, \dots, 8$  and  $j=1$  we form the following systems of linear algebraic equations

$$\begin{aligned}
 1.4\theta_{1,1} - \theta_{2,1} - \theta_{0,1} &= \theta_{1,2} + \theta_{1,0} + 3.939231 \\
 1.4\theta_{2,1} - \theta_{3,1} - \theta_{1,1} &= \theta_{2,2} + \theta_{2,0} + 3.939231 \\
 1.4\theta_{3,1} - \theta_{4,1} - \theta_{2,1} &= \theta_{3,2} + \theta_{3,0} + 3.939231 \\
 1.4\theta_{4,1} - \theta_{5,1} - \theta_{3,1} &= \theta_{4,2} + \theta_{4,0} + 3.939231 \\
 1.4\theta_{5,1} - \theta_{6,1} - \theta_{4,1} &= \theta_{5,2} + \theta_{5,0} + 3.939231 \\
 1.4\theta_{6,1} - \theta_{7,1} - \theta_{5,1} &= \theta_{6,2} + \theta_{6,0} + 3.939231 \\
 1.4\theta_{7,1} - \theta_{8,1} - \theta_{6,1} &= \theta_{7,2} + \theta_{7,0} + 3.939231 \\
 1.4\theta_{8,1} - \theta_{9,1} - \theta_{7,1} &= \theta_{8,2} + \theta_{8,0} + 3.939231 \\
 1.4\theta_{9,1} - \theta_{10,1} - \theta_{8,1} &= \theta_{9,2} + \theta_{9,0} + 3.939231 \\
 1.4\theta_{10,1} - \theta_{11,1} - \theta_{9,1} &= \theta_{10,2} + \theta_{10,0} + 3.939231
 \end{aligned}$$

The above algebraic equations are written in matrix form with I.C and B.C conditions,

$$\begin{bmatrix}
 10 & 1 & 0 & 0 & 0 & 0 & 0 & 0 & 0 & 0 \\
 1 & 10 & 1 & 0 & 0 & 0 & 0 & 0 & 0 & 0 \\
 0 & 1 & 10 & 1 & 0 & 0 & 0 & 0 & 0 & 0 \\
 0 & 0 & 1 & 10 & 1 & 0 & 0 & 0 & 0 & 0 \\
 0 & 0 & 0 & 1 & 10 & 1 & 0 & 0 & 0 & 0 \\
 0 & 0 & 0 & 0 & 1 & 10 & 1 & 0 & 0 & 0 \\
 0 & 0 & 0 & 0 & 0 & 1 & 10 & 1 & 0 & 0 \\
 0 & 0 & 0 & 0 & 0 & 0 & 1 & 10 & 1 & 0 \\
 0 & 0 & 0 & 0 & 0 & 0 & 0 & 1 & 10 & 1 \\
 0 & 0 & 0 & 0 & 0 & 0 & 0 & 0 & 1 & 10
 \end{bmatrix}
 \begin{bmatrix}
 V_{11} \\
 V_{21} \\
 V_{31} \\
 V_{41} \\
 V_{51} \\
 V_{61} \\
 V_{71} \\
 V_{81} \\
 V_{91} \\
 V_{101}
 \end{bmatrix}
 =
 \begin{bmatrix}
 442.2432 \\
 397.5676 \\
 402.0807 \\
 401.6249 \\
 401.6705 \\
 401.6705 \\
 401.6249 \\
 402.0807 \\
 397.5676 \\
 442.2432
 \end{bmatrix}
 \tag{31}$$

Solving the above matrix equation, we get the solutions for changing  $Re=100$   
 $Re=10$   
 $Re=1$

$$\begin{aligned}
 \theta_{1,1} &= 0.4225689 & \theta_{1,1} &= 0.3815506 & \theta_{1,1} &= 0.3477234 \\
 \theta_{2,1} &= 0.2621384 & \theta_{2,1} &= 0.2040747 & \theta_{2,1} &= 0.1815977 \\
 \theta_{3,1} &= 0.12941592 & \theta_{3,1} &= 8.490895 \cdot 10^{-2} & \theta_{3,1} &= 7.499947 \cdot 10^{-2} \\
 \theta_{4,1} &= 0.0567215 & \theta_{4,1} &= 2.9142 \cdot 10^{-2} & \theta_{4,1} &= 2.561393 \cdot 10^{-2} \\
 \theta_{5,1} &= 1.530397 \cdot 10^{-2} & \theta_{5,1} &= 7.483974 \cdot 10^{-3} & \theta_{5,1} &= 7.0066558 \cdot 10^{-3} \\
 \theta_{6,1} &= 3.935121 \cdot 10^{-3} & \theta_{6,1} &= 2.773303 \cdot 10^{-3} & \theta_{6,1} &= 2.386878 \cdot 10^{-3} \\
 \theta_{7,1} &= 1.491726 \cdot 10^{-3} & \theta_{7,1} &= 1.025629 \cdot 10^{-3} & \theta_{7,1} &= 9.620341 \cdot 10^{-4} \\
 \theta_{8,1} &= 5.62172 \cdot 10^{-4} & \theta_{8,1} &= 3.785032 \cdot 10^{-4} & \theta_{8,1} &= 3.356201 \cdot 10^{-4} \\
 \theta_{9,1} &= 2.104959 \cdot 10^{-4} & \theta_{9,1} &= 1.385258 \cdot 10^{-4} & \theta_{9,1} &= 1.03594 \cdot 10^{-4} \\
 \theta_{10,1} &= 7.526057 \cdot 10^{-5} & \theta_{10,1} &= 4.667914 \cdot 10^{-5} & \theta_{10,1} &= 4.181322 \cdot 10^{-5}
 \end{aligned}$$

#### 4. Results and Discussion

##### 4.1. Introduction

The simulation results given focus on the effects of the Ri number and Re number.

##### 4.2. Effects of Re Number on Temperature of Fluid Flow

We solve equation (10) using MATLAB and get the results of the effects of Re number on temperature of fluid as shown in table 1 one below

Distance (L)	Re=100	Re=10	Re=1
0	0.4225689	0.3815506	0.3477234
1	0.2621384	0.2040747	0.1815977
2	0.12941592	$8.490895 \times 10^{-2}$	$7.499947 \times 10^{-2}$
3	0.0567215	$2.9142 \times 10^{-2}$	$2.561393 \times 10^{-2}$
4	$1.530397 \times 10^{-2}$	$7.483974 \times 10^{-3}$	$7.0066558 \times 10^{-3}$
5	$3.935121 \times 10^{-3}$	$2.773303 \times 10^{-3}$	$2.386878 \times 10^{-3}$
6	$1.491726 \times 10^{-3}$	$1.025629 \times 10^{-3}$	$9.620341 \times 10^{-4}$
7	$5.62172 \times 10^{-4}$	$3.785032 \times 10^{-4}$	$3.356201 \times 10^{-4}$
8	$2.104959 \times 10^{-4}$	$1.385258 \times 10^{-4}$	$1.03594 \times 10^{-4}$
9	$7.526057 \times 10^{-5}$	$4.667914 \times 10^{-5}$	$4.181322 \times 10^{-5}$

Table 1: Temperature for varying Reynolds number

The results in the table 1 above is represented graphically as seen in figure 2 below

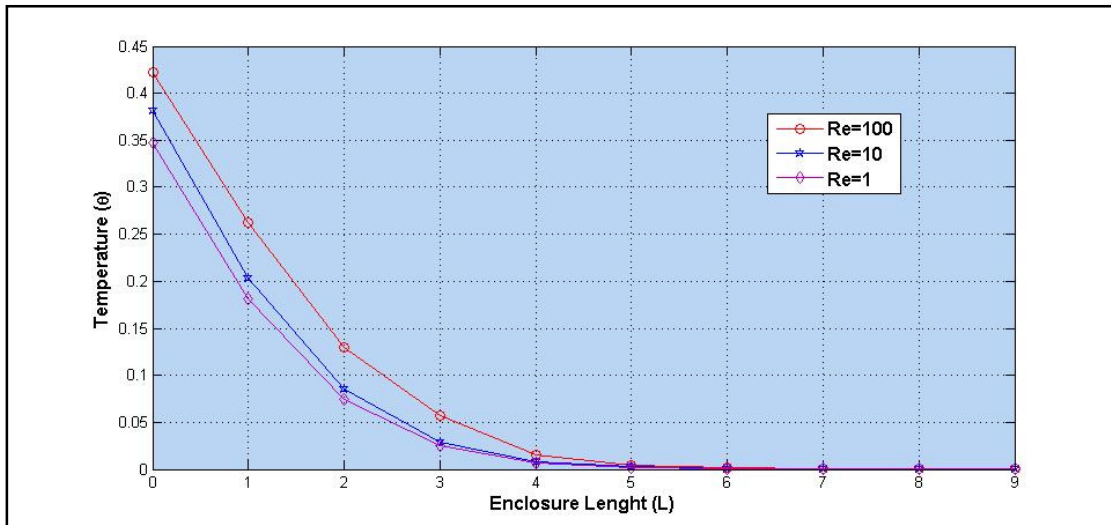


Figure 2: Graph of temperature against enclosure length at varying Re number

At the top of the sliding corrugated hot top surface the temperatures are high as compared to other regions of the enclosure. The velocities are high when the Re was high because the inertia forces dominate over viscous forces. Also at larger value of Re, the effect of buoyancy force become negligible and the fluid flow is governed by the forced convection

4.3. Effects of Ri Number on Horizontal Velocity of Fluid Flow

Distance (L)	Ri=0.8	Ri=1	Ri=2
0	0.7845907	0.7239203	0.4814504
1	0.6446009	0.5657554	0.2489826
2	0.5745702	0.4901801	0.15074
3	0.5431538	0.4570723	0.1107173
4	0.5298703	0.4432731	0.09480941
5	0.5244457	0.437693	0.08859417
6	0.5221927	0.4354089	0.08618175
7	0.520521	0.4338612	0.08513151
8	0.513386	0.4278567	0.08367654
9	0.4574472	0.3812185	0.07446507

Table 2: Horizontal Velocity for varying Richardson numbers

The result Table 2 shows that, as the Ri increases, the velocity decreases. At a given Richardson number, the horizontal velocity decreases as the length of the enclosure increases from the top heating downwards. This is due to the fact that the length of the enclosure increases the kinetic energy of the fluid particles decreases resulting to a decrease in velocity.

The results in the table 2 above is represented graphically as seen in figure 3 below

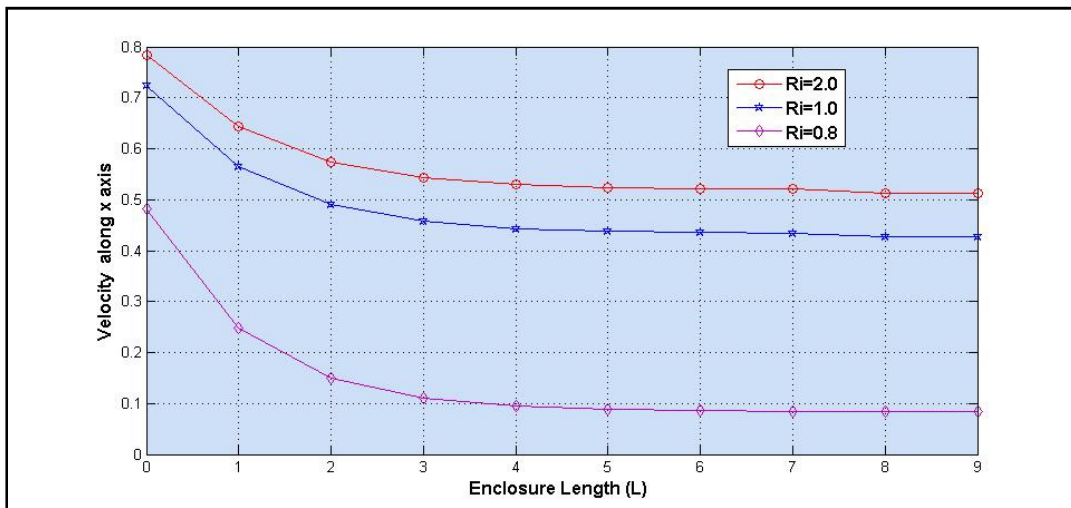


Figure 3: Graph of horizontal velocity against enclosure length at varying Ri number

The effects of  $Ri$  on velocity are shown in Figs. 3 for  $Pr = 6$ . For a fixed  $Pr$ , change of Reynolds number causes the change of Grashof number and hence the Richardson number. On the other hand, at any particular Reynolds number, a significant change velocity flow pattern is marked as the flow regime changes from dominant forced convection to dominant free convection with the increasing  $Ri$ . When  $Ri = 0.8$  forced convection dominate over buoyancy forces. When  $Ri = 1$ , the effects of forced convection balances natural forces. When  $Ri > 1$ , buoyancy forces dominate.

4.4. Effects of Re Number on Velocity along x-axis of Fluid Flow

Distance (L)	Re=1	Re=10	Re=100
0	2.256505	2.751927	3.251927
1	1.800454	2.210618	2.710623
2	1.448099	1.764372	2.264377
3	1.23217	1.473967	1.781872
4	1.041525	1.221808	1.49618613
5	0.8671055	0.9961866	1.17998271
6	0.6930847	0.7799827	0.9858322
7	0.5119629	0.625092	0.7555795
8	0.3407919	0.4685795	0.58581
9	0.1701858	0.2904067	0.3824067

Table 3: Horizontal Velocity for varying Reynolds number

The results in the table 3 above is represented graphically as seen in figure 4 below

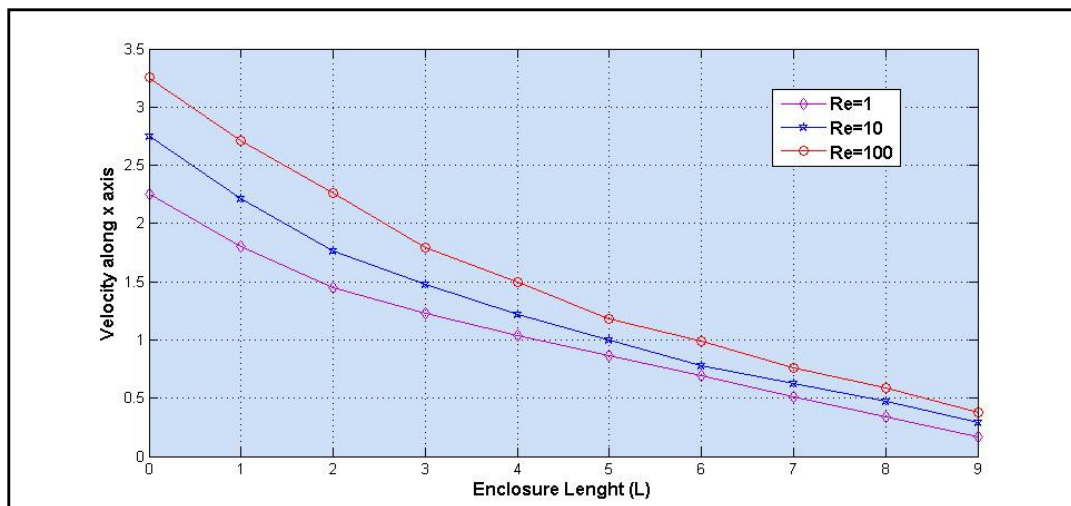


Figure 4: Graph of velocity a long x axis against enclosure length at varying Re number

As the length of the enclosure increased, the horizontal velocity decreased. The viscous forces became dominant. . As the value of Re increased, the inertia forces dominated over the viscous force and the velocity increased.

4.5 .Effects of Ri Number on Vertical Velocity of Fluid Flow

Distance (L)	Ri=0.8	Ri=1	Ri=2
0	1.791321	2.133487	2.475697
1	1.95845	2.404843	2.851606
2	1.982112	2.459012	2.938959
3	1.979277	2.466951	2.955555
4	1.97471	2.465668	2.956911
5	1.97192	2.46386	2.955897
6	1.970272	2.462347	2.954533
7	1.966477	2.457919	2.949393
8	1.940459	2.457919	2.910573
9	1.729321	2.457919	2.59396

Table 4: Vertical Velocity for varying Reynolds number

The results in the table 4 above is represented graphically as seen in figure 5 below

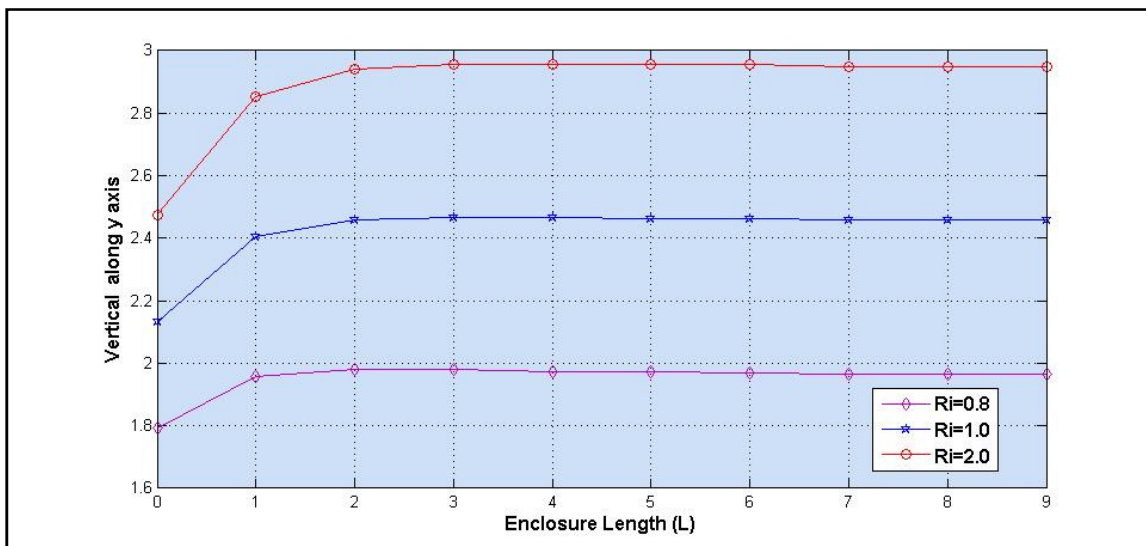


Figure 5: Graph of vertical velocity against enclosure height at varying Ri number

It can be seen from figure 5 that, as the Ri numbers increased the velocity along y axis also increased. As the enclosure length increased, the velocity also increased. The vertical velocity increased up to distance L=2 and then started to decrease for all the three Richardson numbers. This was due to the decrease of the kinetic energy of the fluid particles.

Distance (L)	Re=1	Re=10	Re=100
0	0.2837763	0.2937763	0.3037763
1	0.3631249	0.3731249	0.3831249
2	0.3853104	0.3953104	0.4053104
3	0.3915059	0.4015059	0.4115059
4	0.3932023	0.4032023	0.4132023
5	0.393586	0.403586	0.413586
6	0.393586	0.403586	0.413586
7	0.393586	0.403586	0.413586
8	0.393586	0.403586	0.413586
9	0.393586	0.403586	0.413586

Table 5: Vertical Velocity for varying Reynolds number

The results in the table 4 above is represented graphically as seen in figure 5 below

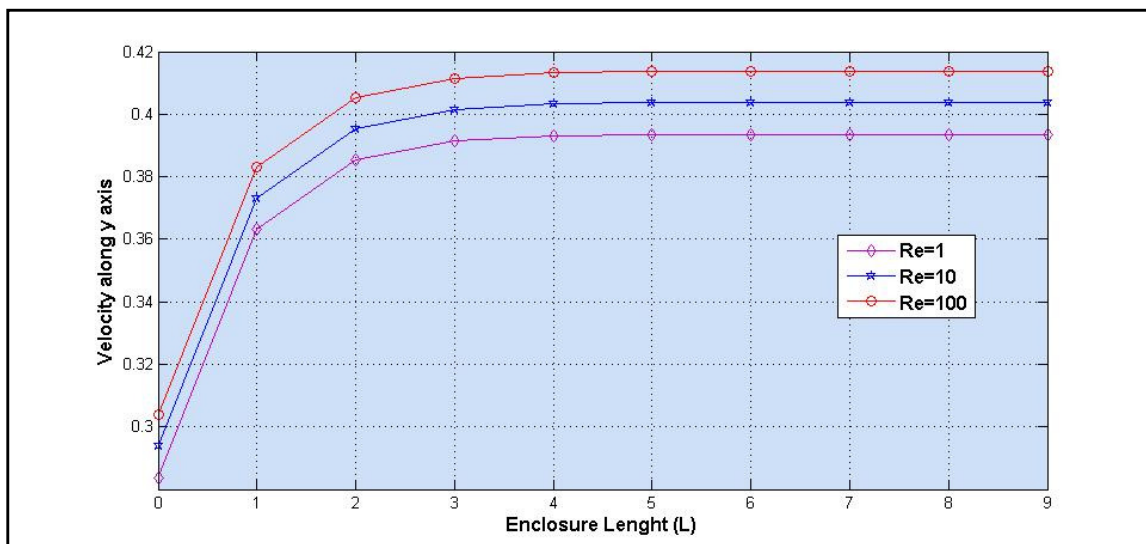


Figure 6: Graph of vertical velocity against enclosure length at varying Re number

It can be seen from figure 6 that, as the Re number increased the velocity along y axis also increased. As the enclosure length increased, the velocity of the fluid also increased. The inertia forces were dominant. As the length of the enclosure increased the viscous forces became negligible, thus the velocity increased.

## 5. Conclusion and Recommendations

### 5.1. Summary

An investigation of heat transfer on combined convection flow was done in a square enclosure with a sliding corrugated hot top surface. The effect of varying the Reynolds, and Richardson numbers were investigated. The nature of velocity profiles and temperature distribution of fluid in the enclosure was studied. The fluid in the enclosure was assumed to be water. The results indicated that when Re was increased velocities on the horizontal and on the vertical increased. The corrugated hot top surface was used to increase heat transfer rate. At the top surface the velocity and temperatures were high. With a lower value of Re, the velocity decreased. When Re was increased the viscous damping action became negligible and the fluid velocity increased. Viscous forces resist the fluid motion. Viscosity in liquids decreases as the temperature increases.

### 5.2. Conclusion

A computational study was performed to investigate the combined convection in a square enclosure cavity with a sliding corrugated hot lid at the top. Results were obtained for  $Ri=0.8, 1$  and  $2$ ;  $Re=1, 10$  and  $100$ . The following conclusions were drawn from the present investigations:

- The forced convection parameter  $Re$  has a significant effect on the flow and temperature fields. When Inertia force was dominant, velocity profiles and temperature distribution was high. The highest velocity and the highest temperature of the fluid was found when the values of  $Re$  and  $Ri$  were high.

### 5.3. Recommendations

Further work is recommended to improve on the results so far obtained for combined convection flow through an inclined square enclosure with a sliding corrugated hot top surface. This may be done by;

- The fluid flow is considered to be non-laminar and steady,  $Re > 2300$
- The fluid inside the enclosure is assumed to be other fluids other than water.

## 6. References

- Ahmed K.H (2010). Numerical prediction of free convection phenomenon through a rectangular inclined cavity filled with a porous media. The Iraq journal for mechanical and material engineering 10 (1):1-21
- Arash K., Seyed S.M and Masoud A. (2014). Using nanofluid in liquid driven shallow enclosure at particular Richardson number: Investigate the effect of velocity ratio. Indian journal of science and technology, 7 (5):698-704.
- Elif B.Ö (2010), Mixed convection in an inclined lid-driven enclosure with a constant flux heater using differential quadrature (DQ) method. International journal of the physical science, 5 (15):2287-2303.
- Hussain S.H (2009), Studying the internal heat transfer by natural convection through an inclined and modified square enclosure with a triangular top wall. Kufa journal of engineering, 1 (1):78-99.
- Hussain S.H (2010), Combined convection flow through inclined rectangular enclosure with sliding wavy hot top surface. International journal of mechanical and material engineering, 5 (2):142-151.

- vi. Khanafer K., Kambiz N. and Marilyr L. (2002), Mixed convection heat transfer in two-dimensional open ended enclosure. *International journal of heat and mass transfer*,45: 5171-5190.
- vii. Kumar L.S, Monotos C.S and Salah K.M.U (2013), Mixed convection heat transfer in a lid-driven cavity with wavy bottom surface. *American journal of applied mathematics*, 1 (5):92-101.
- viii. Mohamed A.T, Ahmed F.E and Enass Z.M (2012), Numerical simulation of double-diffusive natural convective flow in an inclined rectangular enclosure in the presence of magnetic field and heat source. *International journal of thermal sciences*,52:161-175.
- ix. Mohamed A.T, Medhat M.S, Wael M.E and Amr A. (2013), Numerical simulation of double diffusive laminar mixed convective ...in shallow inclined cavities with moving lid. *Alexandria engineering journal*52:227-239.
- x. Mohamed M.K (2013), A numerical simulation of mixed radiation and forced convection heat transfer in a lid-driven cavity filled with participating media. *Journal of basic and applied scientific research*,3 (25):653-665.
- xi. Ntabo O.J., Sigey J.K., Okelo J.A and Okwoyo J.M. (2015), Effect of Electromagnetic Field on Forced Convective Heat Transfer in a Vertical Wavy Channel Divided by a Perfectly Conductive Baffle. *The SIJ Transactions on Computer Networks & Communication Engineering*, 3(3):38-45.
- xii. Obayedullah M., Chowdhury M.M.K and Rahman M.M.(2013),Natural convection in a rectangular cavity having internal energy sources and electrically conducting fluid with sinusoidal temperature at the bottom wall. *International journal of mechanical and material engineering*, 8 (1):73-78.
- xiii. Onchaga C., Sigey J.K., Okelo J.A and Okwoyo J.M. (2013), Turbulent Natural Convection of Heat with Localized Heating and Cooling on Adjacent Vertical Walls in an Enclosure. *International Journal of Science and Research*, 2(10):169-173.
- xiv. Rehena N., Salma P and Alim M.A (2014), Effect of Prandtl number on 3D heat transfer through a solar collector. *International Conference on Mechanical, Industrial and Energy Engineering*,
- xv. Salah U.K.M and Litan K.S (2015) Numerical solutions of 2-D incompressible driven cavity flow with wavy bottom surface. *American Journal of Applied Mathematics*,3 (1):30-42
- xvi. Salam H.H, Khedim H., Mohmoud M.M (2011), Natural convection in a square inclined enclosure with vee-corrugated sidewalls subjected to constant flux heating from below. *Nonlinear analysis modeling and control*, 16 (2):152-169.
- xvii. Sigey J.K., Gatheri F. and Kinyanjui M. (2011), Buoyancy driven convection turbulent heat transfer in an enclosure, 12, JKUAT, Kenya.
- xviii. Stiriba Y., Grau F.X, Ferre J.A. & Vernet A. (2010), A numerical study of three-dimensional laminar mixed convection past an open cavity. *International journal of heat and mass transfer*,53:4797-4808.